

Final Lab: Design and Implementation of a Transduction System for the Measurement of a
Weakly Nonlinear Mechanical Oscillator
ME 310: Instrumentation and Theory of Experiments

Prepared for: Professor Caleb Farny

Prepared by: Owen St. Germain Nathan Smith Martin Dimo

Lab Performed on: October 31st - December 1st, 2022

Report Submitted on: December 5th, 2022

### Objectives of lab

The purpose of this lab is to design and implement a sensor system capable of measuring the position of a mechanical oscillator's top mass. In doing so, this lab aims to apply the information presented in class on second order systems experiencing a sinusoidal input.

Additionally, this lab serves to test the cumulative knowledge from all the previous labs by not providing a step-by-step procedure, but instead requiring the procedure to be generated. All of this combined means this lab will require extensive process development, iteration, and analysis to fully understand the system and data it produces.

# Theory and preparation for analysis

There are quite a few relevant processes that need to be understood in order to properly complete this lab. Firstly, this specific lab group was assigned to the **Linear Potentiometer** pre-selected sensor setup. This setup consists of a long (~80cm), highly resistant, Nickel Chromate wire that has been stretched taut between two extruded aluminum bars vertically. Adjacent to the wire is the oscillator setup, with an additional attachment secured to the top mass of the oscillator. This attachment consists of a plastic exterior and a metal cube with groove cut out of it. This groove rides against the NiCr wire as the top mass of the oscillator moves, providing an electrical contact at any location along the setup.

To utilize this setup as a sensor, it is important to understand **resistivity** and general potentiometer configuration. Every material has a property inherent to its molecular structure that determines how well electricity will flow through it, this is called resistivity. For any given object the total resistance of that object is determined by the resistivity, the cross-sectional area, and the length. NiCr has a particularly high resistivity per unit volume compared to other conductive materials (which is to say, it is not very conductive for a metal). This lab assumes that

the cross sectional area of the NiCr wire is constant throughout its length and a constant composition. Under these assumptions, the only determining factor between two arbitrary points along the NiCr wire is the distance between them. Loading the total length of the wire with some voltage will result in a voltage drop across the entire length of the wire equal to the input voltage, as it is the only resistor in the circuit. Tying it all together, because the resistance between any two points only depends on the distance between them, by measuring the voltage between the ground and wherever the setup interfaces with the wire, some portion of the input voltage can be measured proportional to the length of the wire. In other words, the distance between the bottom of the wire and wherever the top mass is located can be determined by measuring the voltage between their two locations, as seen in Figure 1.

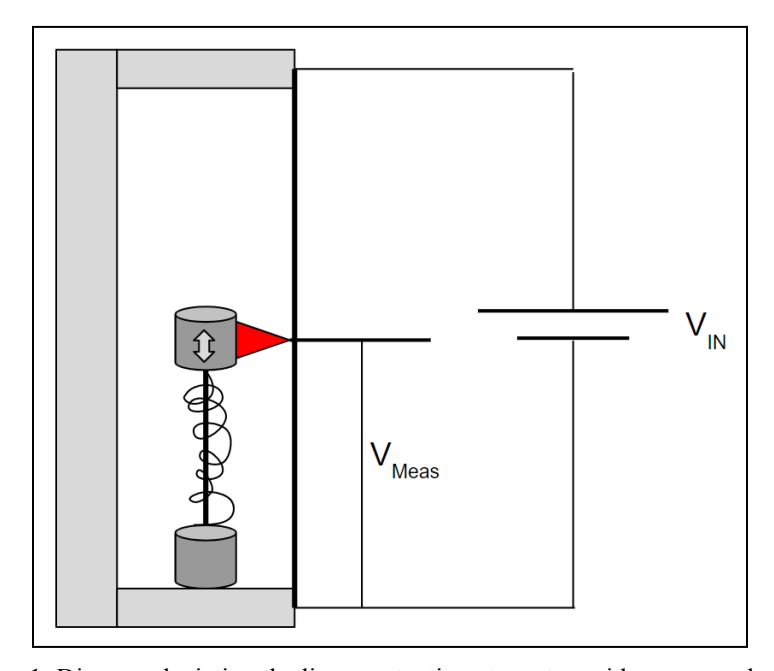


Figure 1: Diagram depicting the linear potentiometer setup with sensor and power

Applying this knowledge is sufficient to get a strong set of data out of the sensor setup, but in order to interpret that data and its relationship to the input, **second order systems** must first be understood. A second order system is characterized by the presence of some oscillatory behavior as part of the system's response to an input. For a system like this lab's linear

potentiometer setup, that inertial behavior comes from the masses of the oscillators. For a second order system, the response to a sinusoidal input also takes a sinusoidal form, with some notable behaviors in addition. Firstly, every second order system has something called a **natural frequency**. The natural frequency is a description of the frequency an undamped system will oscillate at with no additional inputs after the initial stimulus. For an underdamped oscillator, like the ones used in this lab, the natural frequency is difficult to measure directly. To get around this, the **damped natural frequency** can be found instead. This is the actual frequency a system will oscillate at when provided an abrupt input change. That is to say, given a step input, the system will oscillate at the damped natural frequency with decaying magnitude until it reaches a new steady state value. This relationship can be seen in Figure 2, where the response of a system oscillates at its natural frequency before reaching a steady state.

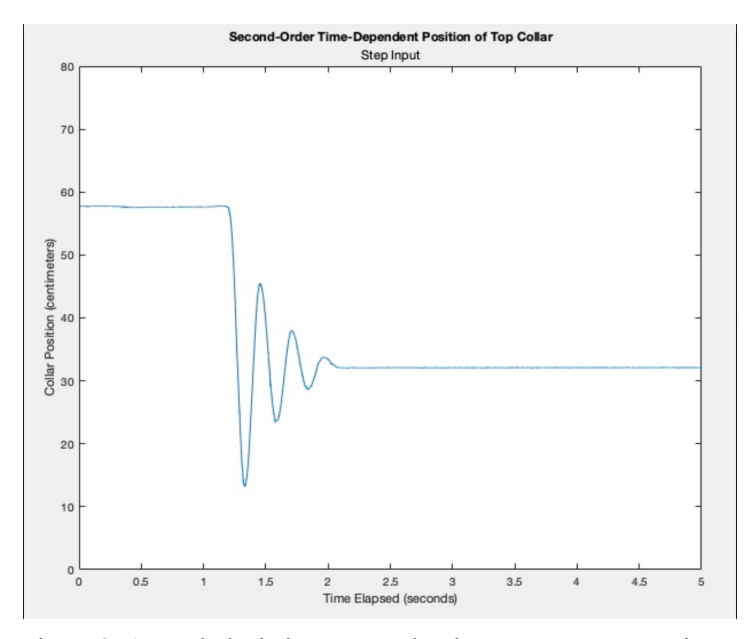


Figure 2: A graph depicting a second order response to a step input

Another important characteristic associated with a second order system is the **damping ratio** of the system. Second order systems that are driven at the same frequency as their natural frequency will experience a large increase in the magnitude of the output. This is a result of the

phase of the input alignment with the phase of the system's natural frequency, creating a system with no destructive wave interaction. The damping ratio describes how much the magnitude of the system's output will grow when the input is driving the system at its natural frequency. This amplitude increase factor is denoted by the frequency dependant variable  $\mathbf{M}(\boldsymbol{\omega})$ . The relationship between a systems damping ratio and the amplitude factor  $\mathbf{M}(\boldsymbol{\omega})$  can be seen in Figure 3.

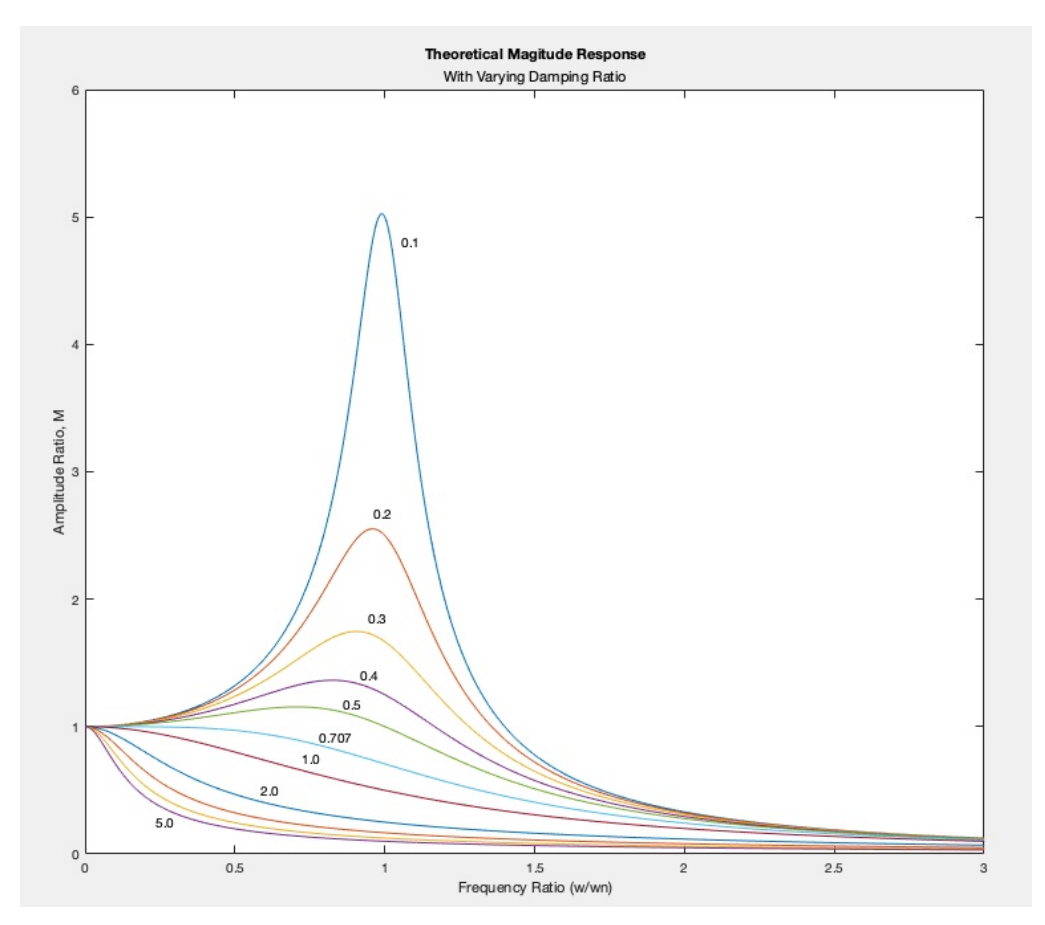


Figure 3: The magnitude of a system's response vs how close to the natural frequency it is being driven

Due to the nature of a second order system, it must have inertia. Thus, the output will take additional time to catch up with what the input is doing due to the time it takes for the mass to accelerate. This delayed response is known as the **phase lag** of the system, and the relationship between the input frequency and the phase lag can be seen in Figure 4. Phase lag manifests itself as a frequency dependent time offset from the input function to the output

function. The output response to a sinusoidal input will be shifted later in time by the phase lag according to the frequency it's driven at.

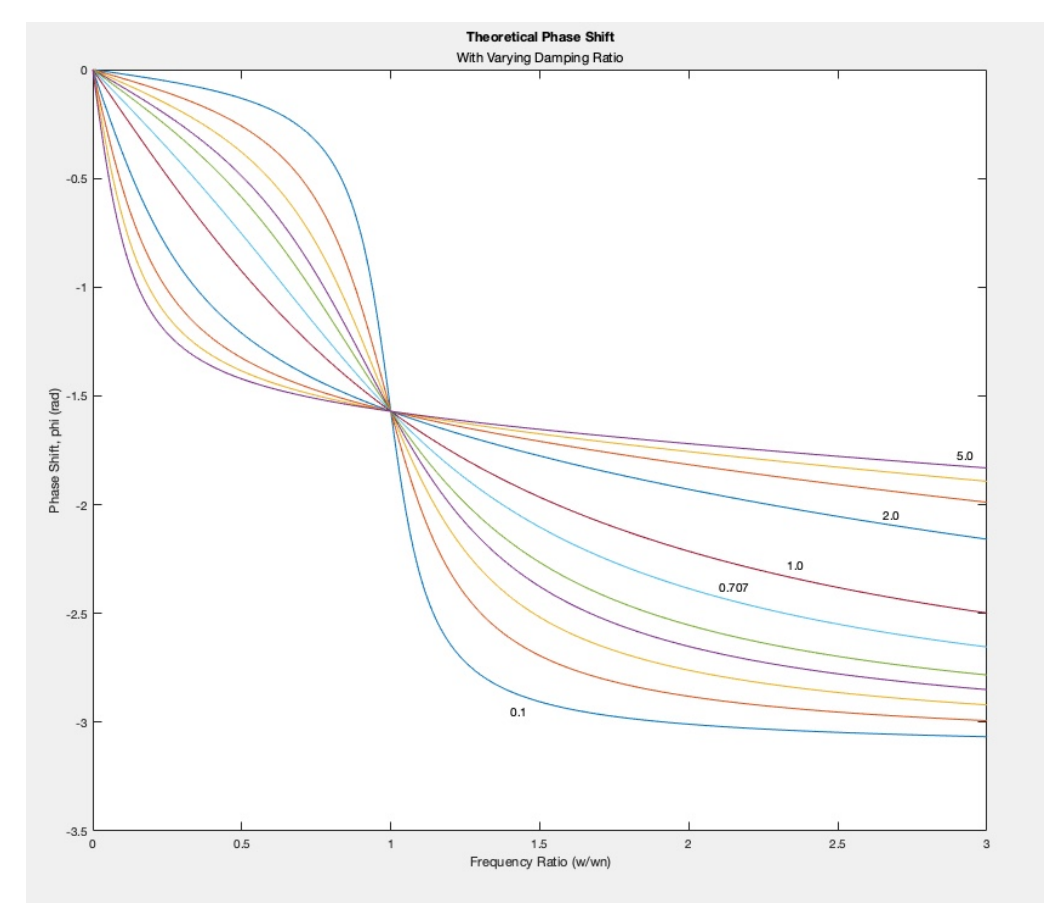


Figure 4: The relationship between frequency ratio to the phase shift

Finally, the relationship between the input frequency and the response frequency is very important to understanding a second order response. A keen-eyed reader would notice that, out of all of the previous parameters listed above, not a single one of them has modified the frequency of the response relative to the input. While the phase lag might shift it around, no part of a second order response actually alters the input frequency provided to it. Thus, the frequency that a second order system oscillates at depends entirely on the frequency of the input provided to it.

### Appropriate tables of symbols and equations

For this lab, nearly all of the equations necessary for the analysis relate to analyzing second order equations. To start, the general form a second order response takes is as follows:

$$y(t) = KX_B M(\omega) sin(\omega t + \phi(\omega) + \phi_0) + KA_0 + O$$
(1)

Where

K = Sensor sensitivity (V/m)

 $X_B = Input magnitude (m)$ 

 $M(\omega)$  = Magnitude ratio (unitless)

 $\phi(\omega)$  = Frequency dependant phase lag (radians)

 $\phi_0$  = Initial phase lag (radians)

 $A_0$  = Input amplitude offset (m)

O = Sensor offset(V)

The values for  $M(\omega)$  and  $\phi(\omega)$  depend on the frequency the system is being driven at, as well as on the damping ratio (which can be seen in Figures 3 and 4 respectively). The equations for these variables are below:

$$M(\omega) = \frac{1}{\sqrt{(1 - (\frac{\omega}{\omega_n})^2)^2 + (2\zeta \frac{\omega}{\omega_n})^2}}$$
(2)

$$\phi(\omega) = -tan^{-1} \left( \frac{2\zeta \frac{\omega}{\omega_n}}{1 - \left( \frac{\omega}{\omega_n} \right)^2} \right)$$
(3)

Where

 $\omega$  = Driving frequency (radians/s)  $\omega_n$  = natural frequency of the system (radians/s)  $\zeta$  = damping ratio (unitless)

 $M(\omega)$  basically describes the factor of how different the response magnitude is to the

input magnitude. Because of this, it can be helpful to understand the difference between the output's magnitude and the input's magnitude. Thus, the dynamic error equation is defined as:

$$\delta(\omega) \equiv |M(\omega) - 1| \tag{4}$$

The damping ratio has several important relationships, but the first is how it interacts with the damped natural frequency ( $\omega_d$ ). This is the system's natural frequency after damping has been taken into account, and is defined as follows:

$$\omega_d = \omega_n \sqrt{1 - \zeta^2} \tag{5}$$

This relationship is quite useful, as the damped natural frequency is the frequency the system oscillates at when introduced to a step input function. That allows  $\omega_d$  to be determined through data by analyzing the peak voltage values of the system's response. Similarly, by analyzing a step response the "envelope" of the step response can be modeled similarly to a 1st order response. This envelope determines the amplitude bounds of the oscillations as the response approaches steady state. This relationship can be modeled as:

$$y_{envelope} = y_{\infty} + (y_0 - y_{\infty})e^{-(t*\omega_n \zeta)}$$
(6)

Where

 $y_{\infty}$  = amplitude at steady state (V)  $y_0$  = amplitude before step input (V)

The important takeaway from this equation is in the exponent. This takes the same form as a first order response, and as a result an effective time constant can be determined for this system:

$$\tau = \frac{1}{\omega_n \, \zeta} \tag{7}$$

$$\tau = \frac{-t}{\ln\left(\frac{y(t) - y_{\infty}}{y_{0} - y_{\infty}}\right)}$$
(8)

Now, with Equations 6, 7, and 4 there are two unknown values (y(t),  $y_{\infty}$ ,  $y_0$ , t, and  $\omega_d$  can all be determined from data collected from a step response) and two equations with which to solve. Rearranging values from Equation 7 and Equation 5, the following relationship can be used to determine  $\zeta$  using just data acquired from a step input response:

$$\zeta = \sqrt{\frac{1}{1 + \omega_d^2 \, \tau^2}} \tag{9}$$

Now, this relationship is useful due to how  $\zeta$  is defined. As the name might imply,  $\zeta$  represents the ratio of how damped the system is to the system's critical damping. This relationship looks like the following:

$$\zeta \equiv \frac{c}{c_{cr}} \tag{10}$$

Where

c = damping constant of the system (Ns/m)  $c_{cr}$  = critical damping of for the system (Ns/m)

The system damping is a variable that depends on the energy dissipation of the system, where the critical damping of the system is defined as:

$$c_{cr} \equiv 2\sqrt{km} \tag{11}$$

Where

k = spring constant of the system (N/m) m = the mass of the system (kg)

Thus, by finding the spring constant, mass, and response to a step input of this system it is possible to combine Equations 11, 10, and 9 to solve for the c.

One more equation involving oscillations is the equation for Q. Q describes the maximum value of the magnitude ratio  $M(\omega)$ , which is when the system is being driven at its resonance frequency. This relationship is useful for determining the damping ratio of the system if the resonance frequency can be found:

$$Q \equiv M(\omega = \omega_r) = \frac{1}{2\zeta\sqrt{1-\zeta^2}}$$
(12)

The last relevant equation to this lab does not relate to a second order system, but instead describes how a linear potentiometer works (discussed in the Theory section above). The resistance of a given object is determined by the resistivity equation:

$$R = \rho \frac{L}{A} \tag{13}$$

Where

L = length of object (m) A = Cross-sectional area of object (m<sup>2</sup>)  $\rho$  = resistivity of the material ( $\Omega$ m)

While the actual resistance value is not necessary to calculate for this lab, this equation is important to understanding the procedure and the system as a whole.

## **Equipment lists**

<b>Equipment Name</b>	Manufacturer	Model	Resolution	Range
Data Acquisition Board	National Instruments	PCI-6221	0.00015 V	9.8 V
Linear Potentiometer Oscillator	Boston University	ME310 #1	0.0001 m	3.82 Ω
Power Supply	Agilent	E3631A	0.001 V	0-6V/0-25V
Multimeter	Keysight	34461A	10 MHz	0.1V to 1 kV
Meter Stick	Johnson	M391/40-0560	+/- 0.0005m	1m

**Table 1**: List of equipment used durn the lab and their respective resolutions and ranges

### **Methods and Materials**

For this lab, three different sensor configurations were trialed until a sensor with sufficient accuracy was produced. The first setup involved creating a Wheatstone Bridge and using the resistance from the potentiometer as one of the legs in the bridge. This caused several issues however, as balancing the bridge at steady state required three additional resistors. With these additional resistors, even trying to read a signal at steady state produced a graph with unpredictable values, and a seemingly random slope. Ultimately, due to this setup's low relative sensitivity, high signal to noise ratio, and complex setup requirements the Wheatstone Bridge design was scrapped.

The second design iteration for this lab opted to remove two of the resistors to create a voltage divider circuit between the potentiometer value and another resistor. Balancing this setup did prove easier than the Wheatstone Bridge, but still came with its own problems. Most notably, as part of this setup, the voltage across the constant resistor was being measured, not the voltage

across the potentiometer. This meant that any change in resistance of the potentiometer was only felt in the sum of the two resistances values for this configuration. Given the small magnitude of the potentiometer's resistance changes  $R_1 + R_2 + \Delta R_1 \approx R_1 + R_2$ . This also created a situation where, even at steady state, the measured values of this sensor were random and non-constant, likely as a result of noise.

After multiple trails of unusable data, the third and final experimental setup was determined. This setup (seen in Figure 1) uses just the resistances measured across a portion of the potentiometer. By applying a voltage across the two ends of the NiCr wire, the voltage drop across this wire is equal to the total voltage applied to it (assuming negligible added resistance from other connections). This means that by measuring the voltage between the ground point and wherever the top mass of the oscillator is connected, the voltage drop will be proportional to the distance between them. This also means that the full scale voltage of the sensor is directly controlled by the applied voltage across the entire wire. This means that a higher input voltage would actually produce a larger sensitivity value (with diminishing returns). With that being said, there are some safety limitations. Since the entire potentiometer necessitates an exposed wire, feeding the setup with a large voltage value could potentially draw a dangerous amount of current. Keeping that in mind, this lab opted for an input voltage of 2V. This generated data that was magnitudes better than the previous two configurations, and stayed near constant at steady state. Because the data was so smooth, a hardware filter was determined to not be necessary.

The voltage values produced by this setup were fed via a BNC connector into the DAQ Board, which was then used to record data. With this setup, the board was set to record at 100kHz for 5 seconds, producing 500,000 data points. Figure 5 shows this configuration as a block diagram, with values for the sensor parameters found later in this lab.

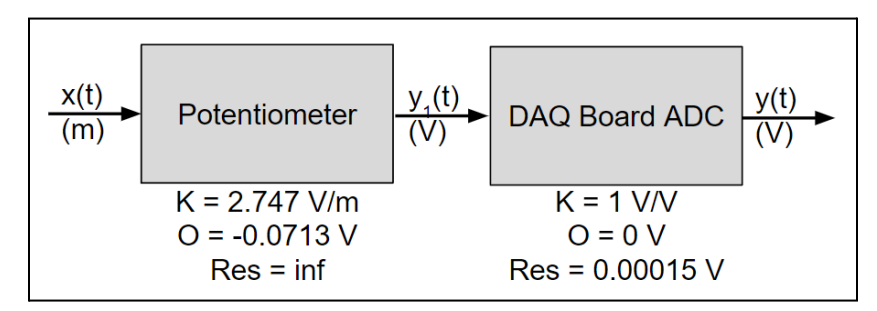


Figure 5: Block diagram of the lab's sensor setup

With the experimental setup solidified, there are three main processes required to properly analyze this system. The first procedure is to calibrate the system. The goal of these steps is to find the relationship between the voltage measured and the actual position of the top mass. Additionally, this data can also be used to determine the spring constant of the system.

To begin, the initial data acquisition should be done while the system is at steady state. This provides the onloaded (except by gravity) position of the system. While unloaded, use a meter stick to measure the distance between the top of the topmost mass and some fixed point (this lab referenced the black base plate). Next, hang a 200g mass from the top mass and allow it to displace the mass and reach a steady state. While resting at this new steady state, record another set of 500,000 data points, and measure the new height with the meter stick. The extremely high quantity of data recorded for each trial effectively negates the effects of any outliers/random noise in the data. This is reflected in the uncertainty values later on in this lab. Repeating this loading procedure many times with different masses will result in several important details of the system. Converting the masses into weight, the applied force to displacement relationship from this procedure can be used to calculate the spring constant of the system, k. Additionally, using the mean voltage for each steady state position allows a

relationship between voltage and position to be generated (discussed further in the Analysis section).

The second procedure for this system is useful for characterizing the oscillatory properties of the system. To start, the system should be connected to the DAQ board and Power Supply as in the previous procedure. For this procedure, the first step is to hold the top oscillator at some position away from its equilibrium resting position (high or low are both valid). While the top mass is being held, start the data acquisition process and wait approximately two seconds. After two seconds, release the mass from its current position and allow it to return to equilibrium. Repeat this process at least three additional times, though more data will result in a smaller uncertainty value. The value of this procedure is that it showcases the system's damped natural frequency as the system reacts to a step input. This damped natural frequency would otherwise be quite difficult to model, so finding it experimentally is extremely helpful to start analyzing the system.

The final procedure is used to gather experimental data for the system's response to a sinusoidal input. With the oscillator hooked up to the DAQ Board, start the input motor at 5% power. Once the output has reached a steady state oscillatory response, start the data acquisition and allow it to record for the full five seconds without interruption. Save this data set using a labeling system that differentiates what power setting the input was set to, as well as if the previous trial was a higher or lower value (for hysteresis analysis). After collection, increase the power setting of the input by another 5% and repeat the acquisition. Notably, as the magnitude of the response starts to get quite large, the power incrementation between trials should decrease from 5% to 2% until the amplitude decreases again. This will provide a better resolution around the resonance frequency, and help analysis in the future. Additionally, making sure the wires

have enough slack while oscillating is *extremely* important to getting good results, as a taut wire will frequently break connection or introduce extra noise into the data. Once the output has been measured at 100% power, start reducing the power in increments of 5% per trial all the way back down to 5%.

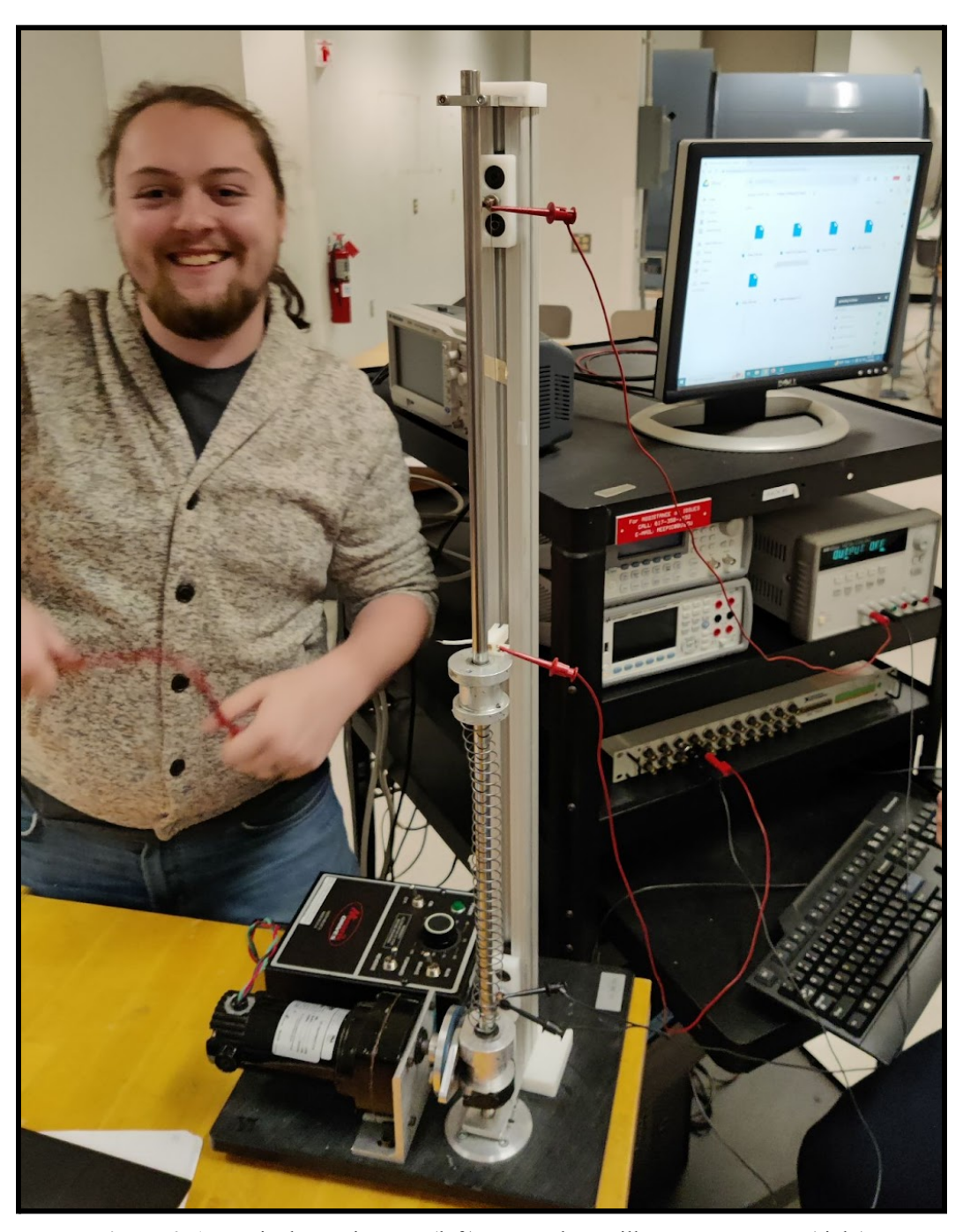


Figure 6: An excited experimenter (left) next to the oscillator system setup (right)

# In-Lab Notebook

							₹ 24 2
	Equip	went Liot	-ab Pro	ject			
	Mass	: 126.950					
	Spring	Equipment	ita a si				
	Decad	e Besistance	ith resistance : Nox: Tenna	1 E 310 #1			
	Radh	#5	lenma	72-7270			
	Total	Samples: 5	0.000				
	Power	5V	0,000				
	Data	)					
				1013			1
		368	2 oscilloscope	set value	6.32 SL		
1815	(5	7 3 #1	Thing				
		3	111/19		376293 EIN TAV	, 10/	
				1,100	S TN IHV	JAIN	
	Initio	al Setup v	ich we.e.				d
	Maca of	weight: 12	6.960				
				ma mace to	to fore	of top: 36.	6.
			Total Load (N)		top race	07 10p. 50.	SCW
	201a	33.5 cm	3.217N	0.03m	107.23		1
		30.4cm	6.160N	0.06lm	100.98		d
	501g		8.132N	0.087m	93,47		d
	( )	27.8cm	10.094N	0.\09m	92.26		
	9029	25.6cm	11.085N	0.115	96.39		3
	10039	25.0cm	11.0000	10.110			
			C . ( C .	-7 C-1	O4 Direct	ion Ss, Chan	0019
	Calibro	ation	FS: [-5,!	JI-T CC	AV6 V	STOEY	mc(2
	Height /	Aug 1 51	rdev	Height		Total Control of the	
4	36.5	2006 2	803.10	20.45	2.6702	0.0041	7
	31.8	9 906 F	0849.10	20.45	2.6646	0.0017	
	26.05	0 ( (1)   5	1948-104				
		0 7000 141	274,10				
1	- , , ,	2,7789 5	4668,10-4				23
	31.05	طرا				W. 111 Tax	
			-	A		The state of the s	

0	11/10/22 New setup	₹ 25
	New setup	
Mass (g)	Position Measured 1/21	
0	100	
200	1000 1012	
400	1205	
600	12902.10-4	
800	0.4505 13948,104	
1000	33 9 0.6681 1.1920.10-4	
	33.4   0.6339	
	Distance from plate to input mass top face: 8.1cm	
	At max height: 14.5	
Percent		
10	tage # of input cycles	
20	7.2	
30		
71		
	Period = los	
4		
5.		
6		
7	70	
4	50	
9	NO NO	1
10	00	- A

<b>E</b>		₩ 26
0		
	Sample Calculations	
	Whitesterney Calibration:	
	$V_{p,i} = 1 t_{v,45\%} \frac{5y}{\sqrt{N}} = 11.96 \cdot \frac{0.00013362}{\sqrt{500000}} = 0.0000003704$	
	$w_{i} = \frac{1}{V_{p,i}^{2}} = \frac{1}{(0.0000003704)^{2}} = 7289789475731$	
	(0,000000 5/04)	
	w; x;2 = (72 89783475731)(0356)2 = 923878632260	
	Wiymi = (7289788475731)(0.9072) = 6613296105183	
	W;x; = (7289788475731)(0.356) = 2595164697360	7
	Wixigni = (7289788475731) (0.356) (0.9072) = 2354333413445	4.5
	Fir Bw = Σω; Σω; x; 2 - (Σω; x;)2 = (47141021841167) (440739489190) = 2.88 × 1024	( 127,
	Q = Σω; x; 2 Σω; ym; - Σω; x; Σω; x; jm; - (4,4(x,0)2)(3.6×1013)-(1.43)	(1013) (1.11 x1013)
	Bw 2.88x(02	1
	= -0,07196V	
	d = Zw; Zw; xigm; - Zw; x; Zw; yym; - (4.71x1013)(1.11x1013) - (1.43x1013)  Bw 2.88x1024	(3.6×10/3)
	Bw 2.88x1024	P A
	= 2.747 N/m	
	Enverted a : de 0.07196V :00 02596.	
	Inverted as: de = -0.07196V :0.02596m	
	Invested a, = = = = = = 0.364 m/V	
	4, 2.741 V/m	
	$y_{sit} = x_i \cdot a_i + a_0 = (0.356)(2.75 \text{Vm}) - 0.0713 \text{V} = 0.9065 \text{V}$	
	9517 - 2, 2, 440 - 6.000 (2.17)	
	Syx = - \[ \sum_{\text{E[y5it-3meas}}^2 = \sum_{\text{yqqqq8}} = 0.000003058 \]	
	1 499998 = 0.00005050	
7	Up.yfit = 5x · tr. 95% = 0.000003058 · 1.96 = to.00000 599 V [96%]	=

# **Analysis**

All sample calculation screenshots shown in this section and the Uncertainty Section are taken from the In-Lab Notebook section. All sample calculations performed in this section utilize the first trial values from the data tables. In this lab, the first step of interpreting the data was calibrating the system. To achieve this, a weighted calibration was performed as shown below.

	Mass (g)	Position (m)	Xi - Position (m)	Ymi - Meas Voltage (V)	STDEV	Up	wi	(wi(xi^2))	wiymi	wixi	wixiymi	yfit (V)	(yfit - ymeas)^2
	0	0.437	0.356	0.9072	1.34E-04	3.70E-07	7.29E+12	9.24E+11	6.61E+12	2.60E+12	2.35E+12	0.907	4.76E-07
	200	0.422	0.341	0.8633	1.31E-04	3.62E-07	7.63E+12	8.87E+11	6.59E+12	2.60E+12	2.25E+12	0.865	4.04E-06
	400	0.395	0.314	0.7919	1.29E-04	3.58E-07	7.82E+12	7.71E+11	6.19E+12	2.46E+12	1.94E+12	0.791	5.61E-07
	600	0.38	0.299	0.7505	1.39E-04	3.87E-07	6.69E+12	5.98E+11	5.02E+12	2.00E+12	1.50E+12	0.750	3.01E-07
	800	0.349	0.268	0.6681	1.19E-04	3.30E-07	9.16E+12	6.58E+11	6.12E+12	2.45E+12	1.64E+12	0.665	1.09E-05
	1000	0.339	0.258	0.6339	1.23E-04	3.42E-07	8.55E+12	5.69E+11	5.42E+12	2.21E+12	1.40E+12	0.637	1.18E-05
	500	0.007	0.000	0.70045		0.505.07	7.005.40	7.055.44	5.005.40	0.005.40	4.055.40	0.700	4.005.00
Avg:	500	0.387	0.306	0.76915	1.29E-04	3.58E-07	7.86E+12						4.68E-06
Sum:							4./1E+13	4.41E+12	3.60E+13	1.43E+13	1.11E+13		
												Syx:	3.06E-06
	Bw	2.88E+24		Position Fit	Upper	Lower						Upyfit (V):	5.99E-06
	a0	-0.071296	V	304.34	304.34	304.33						Upxfit (mm):	2.18E-03
	a1	2.746646	V/m	288.35	288.36	288.35						Ub,1 (res) (V):	7.50E-05
				262.36	262.36	262.36						Utotal (V):	7.52E-05
	Inverted			247.28	247.29	247.28						Utotal (mm):	2.74E-05
	a1	0.364080	m/V	217.28	217.29	217.28							
	a0	-0.025957	m	204.83	204.84	204.83							

**Table 2:** Raw data, calibration terms, and fit values used during the calibration process

For calibration, six different masses (0g, 200g, 400g, 600g, 800g, 1000g) were placed on the spring mass. The position of the spring mass was measured with a meter stick. The voltage was measured at this position through the linear potentiometer at 500000 samples for 5 seconds. The mean voltage and standard deviation was automatically calculated via the script used to collect them. These measurements are shown in Table 1 next to the position data. Table 1 contains all the calculations performed to calculate the slope (a<sub>1</sub>) and y-intercept (a<sub>0</sub>) values of the linear calibration curve. These values were also inverted to be able to later convert the measured voltages to a position on the potentiometer. The following sample calculations were performed to get the linear fit constants, a<sub>0</sub> and a<sub>1</sub>.

	Wholegraphy Calibration:	
	Up; = 1 ty, 45% W = 1   .96 . 0.000 3362 = 0.0000003704	
		1
	$w_i = \frac{1}{V_{ei}^2} = \frac{1}{(0.0000003704)^2} = 7289789475731$	4
		4
	w; x;2 = (72 99789475731)(0356)2 = 923878632260	
	Wiyni = (7289788475731)(0.9072) = 6613296105183	4
	W;x; = (7289788475731)(0.356) = 2595164697360	
-	Wix; yni = (7289788475731) (0.356) (0,9072) = 2354333413445	
	Fix Bw = Ew; Ew; x; 2 - (Ew; x;)2 = (47141021841167) (440739489194	2)-(14313991969
	= 2.88×10 <sup>24</sup>	127/2
	a <sub>0</sub> = Σω; x; <sup>2</sup> Σω; ym; - Σω; x; Σω; x; ym; - (4.4(x,0 <sup>2</sup> )(3.6x,0 <sup>3</sup> )-(1.43x)	1013) (1.11 x1013)
	Bw 2.88x(024	
	= -0,07196V	
	a, = Zw; Xv; x; ym; - Zv; x; Zv; yym; - (4.71x1013)(1.11x1013) - (1.43x1013)  Bw 2.88x1024	(3.6×10/3)
	= 2,747 N/m	
	Inverted as: de0.071960 _ 10.02596m	
	Inverted $a_0$ : $\frac{d_0}{a_1} = \frac{-0.07196V}{2.747 \text{ V/m}} = \frac{-0.02596 \text{ m}}{2.747 \text{ V/m}}$ Inverted $a_0$ : $\frac{1}{a_1} = \frac{1}{2.747 \text{ V/m}} = 0.364 \text{ m/V}$	

Mass of	weight; 12	6.96g			
Distan	ce from to	p face of botton	m mass to	top face of to	p: 36.5cm
Load	Distance		∆x <b>&amp;</b>	K	
201a	33.5 cm	3.217N	0.03m	107.23	
	30.4cm	6.160N	0.061m	100.98	
7029	27.8 cm	8.132N	0.087m	93.47	
	25.6cm	10.094N	0.\09m	92.26	
9029	25.0cm	11.085N	0.11500	96.39	
1003g	20.00	1,,,,			

 Table 3: Raw data used for calculating the spring constant

For calculating the spring constant, we used five masses (201g, 501g, 702g, 902g, 1003g) to place on the spring mass. The initial height and final height of the spring mass was measured

as  $\Delta x$  in Table 3. The total load was calculated by multiplying the total mass (spring mass + added mass) by the acceleration due to gravity (9.8m/s<sup>2</sup>). The spring constant was calculated by dividing the total load by the  $\Delta x$ . The final spring constant values are displayed in the last column of Table 3.

Since the potentiometer sensor isn't detachable from the upper collar, the output of second-order motion, the characteristics of the input, or bottom collar, needed to be calculated from the behavior of a step input. The step input responses allowed for an envelope analysis to be performed, resulting in system parameters such as the natural frequency and damping ratio. For redundancy, the envelope analysis was performed through two different methods; one through Matlab and the other on Microsoft Excel. In both analyzes, the output data of the step input runs were manipulated to find the varying decaying amplitude.

Starting with the Matlab variation; our different runs were analyzed, each with a different initial state, resulting in four different output responses as displayed in Figure 7. Due to the clean nature of the data, no filtering was necessary for this specific analysis. Next, the mean value of the final position, or steady-state voltage, was retrieved from the data by only using the time range between four and five seconds after data acquisition began. This mean value was then used to normalize the output response onto the x-axis, upon which the absolute value of the data was taken to have more peaks, and thus more data points for the envelope analysis, which is displayed in Figure 8. The "findpeaks" function is then applied to the manipulated data to find an oscillation period and exponential envelope slope, which is defined by Equation 7. The slope, referred to as tau, has two unknowns, which are the same unknowns in Equation 5. With this in mind, the system of equations composed of Equation 5, Equation 7, and the natural frequency and damping ratio is able to be solved.

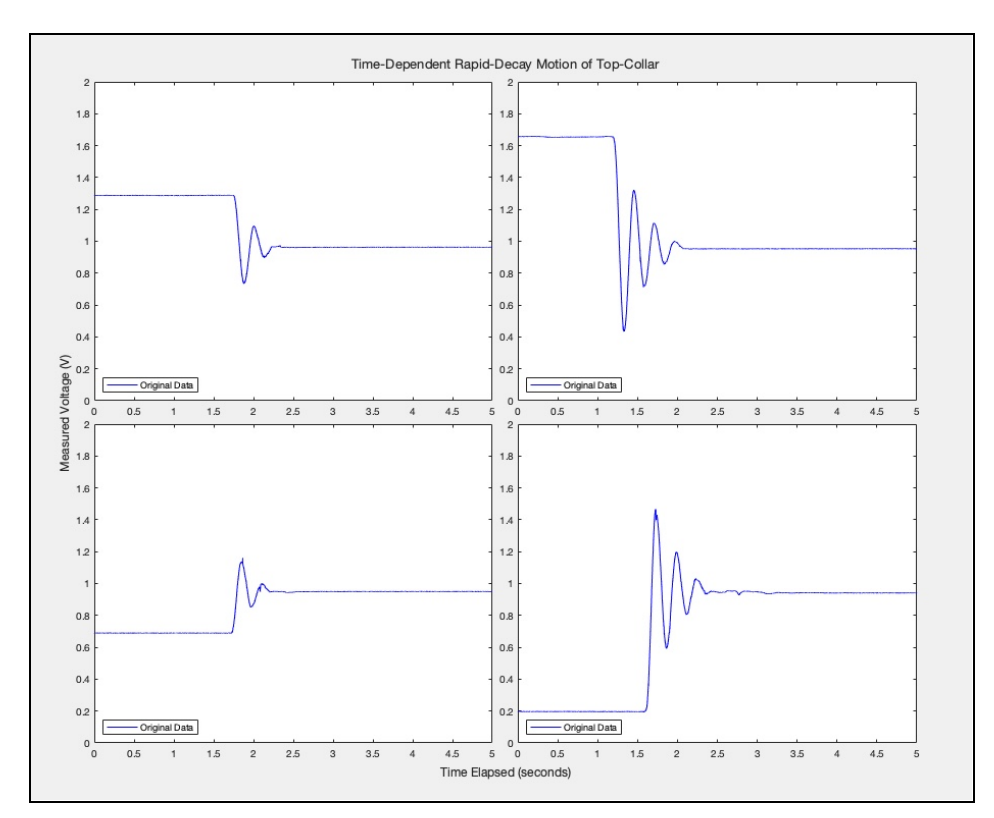


Figure 7: An overlay of all step-input responses as a function of time

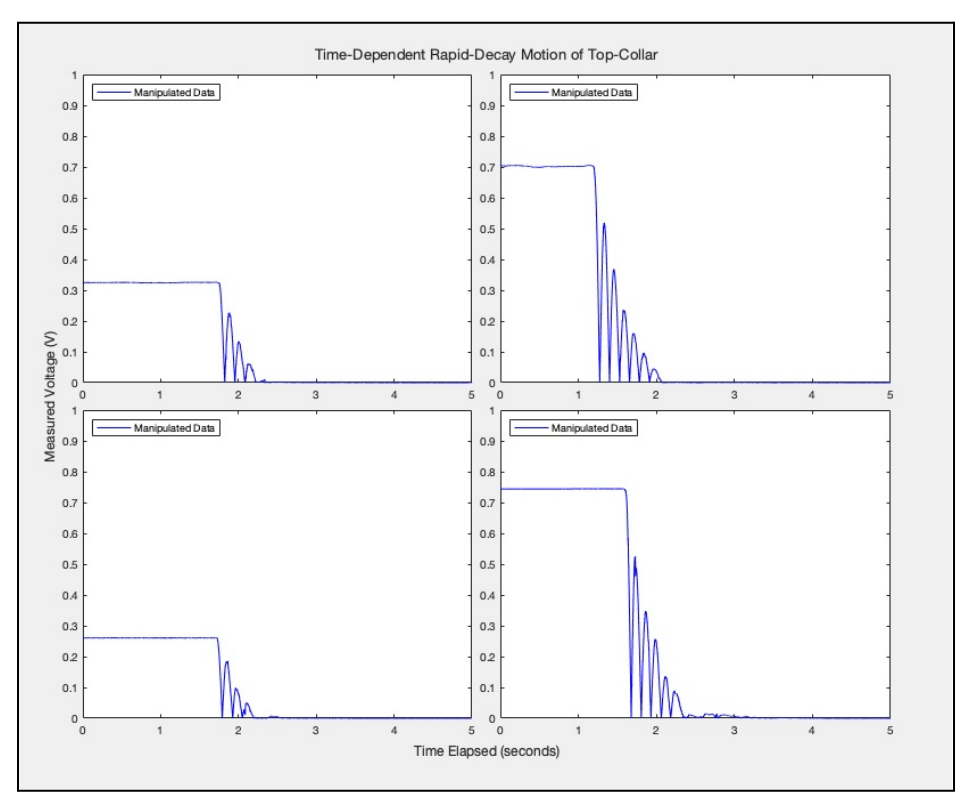


Figure 8: The manipulated step-response functions for peak analysis

Similarly, the step function analysis through Microsoft Excel solved for the same system of equations consisting of Equation 5, Equation 8, and Equation 9.

High 1					High 2				
Time (s)	Position (m)	Adjusted Position (m)	t	Tau	Time (s)	Position (m)	Adjusted Position (m)	t	Tau
1.881	0.2411	0.4075	0.132	0.372	1.332	0.132	0.51	0.147	0.486
2.005	0.3734	0.3734	0.256	0.290	1.452	0.4552	0.4552	0.267	0.414
2.134	0.3001	0.3485	0.385	0.242	1.585	0.2358	0.4062	0.4	0.364
					1.704	0.3797	0.3797	0.519	0.353
					1.84	0.2858	0.3562	0.655	0.330
Yinf:	0.3243				Yinf:	0.321			
Y0:	0.4429				Y0:	0.5767			
Drop Time:	1.749				Drop Time:	1.185			
Average T:	0.253				Average T:	0.254			
wd:	24.83				wd:	24.73695003			
Low 1					Low 2				
Time (s)	Position (m)	Adjusted Position (m)	t	Tau	Time (s)	Position (m)	Adjusted Position (m)	t	Tau
1.849	0.3871	0.2533	0.127	0.361	1.726	0.5079	0.1317	0.136	0.345
1.965	0.2838	0.2838	0.243	0.253	1.862	0.1896	0.1896	0.272	0.357
2.107	0.3384	0.302	0.385	0.233	1.987	0.4102	0.2294	0.397	0.352
					2.117	0.267	0.267	0.527	0.317
					2.232	0.35	0.2896	0.642	0.289
Yinf:	0.3202				Yinf:	0.3198			
Y0:	0.2251				Y0:	0.04085			
Drop Time:	1.722				Drop Time:	1.59			
Average T:	0.258				Average T:	0.253			
wd:	24.35343142				wd:	24.83472453			
Average Tau:	0.335								
Average wd:	24.69								
wn:	24.8698159								
Damping Ratio:	0.120048653								

Table 4: Raw data, intermediate calculations for the time constant (tau), damped natural frequency  $(w_d)$ , natural frequency  $(w_n)$ , and damping ratio.

After collecting the data as shown in Figures 7 and 8, values were put into Excel to perform the necessary calculations to solve for the resulting natural frequency and damping ratio. The time constant value ("Tau" in Table 4) for each peak was calculated using Equation 8. The time constant values for all peaks of all four test trials were averaged to get an average time constant value of 0.335s. For each of the four test trials, the damped natural frequency was calculated by converting the period between two peaks from seconds to radians/second. After averaging the damped natural frequencies for all four trials, the damping ratio was calculated

using Equation 9 by using the average damped natural frequency and average time constant. The natural frequency was then calculated using Equation 5. These calculations are shown in the sample calculation below.

$$\mathcal{T} = \frac{-t}{\ln(\frac{3t-3\sigma}{3p-3\sigma})} = \frac{-0.132s}{\ln(\frac{0.4075m-0.3243m}{0.4429m-0.3243m})} = 0.372s$$

$$w_d = \frac{2\pi}{T} = \frac{2\pi}{0.253s} = \frac{24.8 \text{ rad/s}}{1-5^2}$$

$$w_n = \frac{w_d}{\sqrt{1-5^2}} = \frac{24.69}{\sqrt{1-(0.12)^2}} = \frac{24.87 \text{ rad/s}}{1+(24.69)^2(0.335)^2} = 0.12$$

A third method used to determine the damping ratio related to the sharpness of resonance, commonly noted as the quality factor, Q. This parameter is defined in Equation 12 and relates the maximum amplitude ratio to the damping ratio. By utilizing our data at maximum amplitude, which was determined visually on the day of data collection, a quick calculation was performed to gather another unique value for the systems' damping ratio for sake of redundancy and cross-referencing. A sample calculation for this calculation is shown below.

$$Q = M(w_r) = \frac{1}{25\sqrt{1-5^2}}$$

$$6.3443 = \frac{1}{25\sqrt{1-5^2}}$$

$$S = 0.07405$$

As shown in the sample calculation below, the damping constant (c) was calculated using equation 10 (with a substitution of Equation 11). The damping constant was calculated to be  $0.847 \text{ N}^2\text{s}^2/\text{m}^2$ .

$$C = 25\sqrt{mk} = 2(0.12)\sqrt{0.12695kg} \cdot 98.066N/m = 0.847N^25^2/m^2$$

Upon completion of the analysis of system parameters, the main sinusoidal data was interpreted resulting in experimental amplitude ratios across a wide frequency range. To acquire the magnitude data out of the system response, the sinusoidal amplitude was needed, which was extrapolated using Matlab.

The first step involved visually inspecting the collected data sets from the potentiometer, ranging from 10% power to 100% power in increasing and decreasing increments. In Figure 9. the raw output can be visualized for a five second data acquisition period at 60% power (the corresponding natural frequencies that correlate with each system power step are determined by the calibration process and are referenced in the Results section). Moving forward, all sample plots show the applied analysis to only the 60% power data, but it can be assumed that all processes were carried out to all data sets for accurate results.

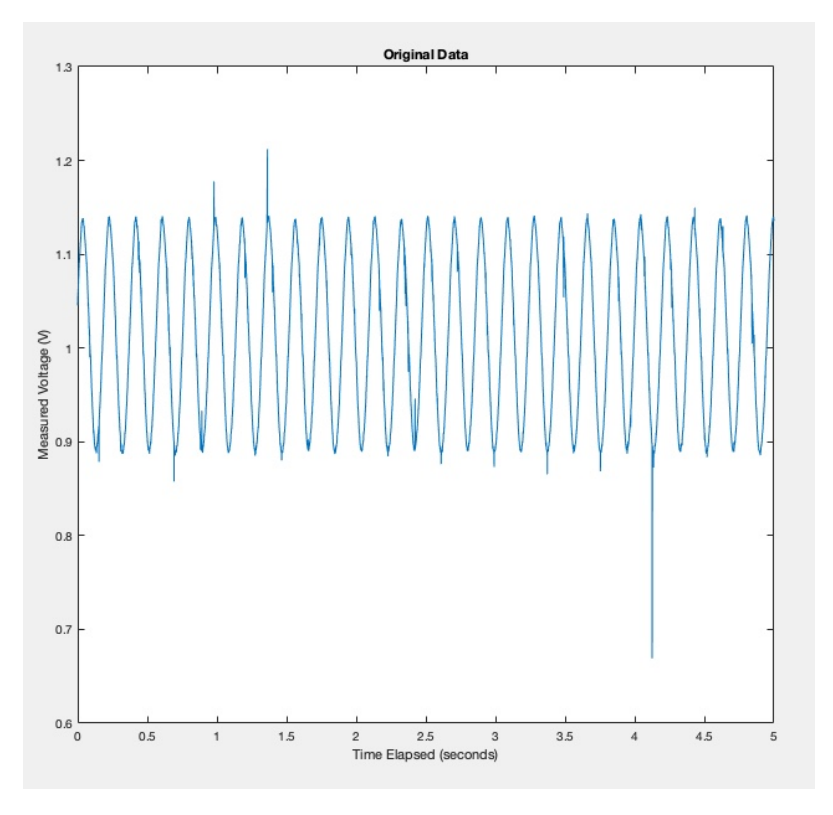


Figure 9: The raw position-output of the potentiometer in Volts

As can be seen, the raw data isn't as "clean" in terms of signal noise as deemed acceptable for amplitude analysis. The far outliers on both extrema represent a physical loss of contact between the potentiometer wire and variable bar, resulting in large spikes. Due to an impurity in the wire closer to the lower end of its range, its plausible to relate the largest of these outlier points to this physical anomaly.

To clear these outliers analytically, a "hampel" filter is used. Found within the Matlab definitions, the "hampel" filter is a variation of windowed length parameter identifier, that calculates the median and standard deviation within a given window or range. If an outlier exceeds the standard deviation threshold of the given window, its value is replaced by the calculated median value. This filter effectively cleared the physical noise that was recorded by the potentiometer and resulted in a graph shown in Figure 10.

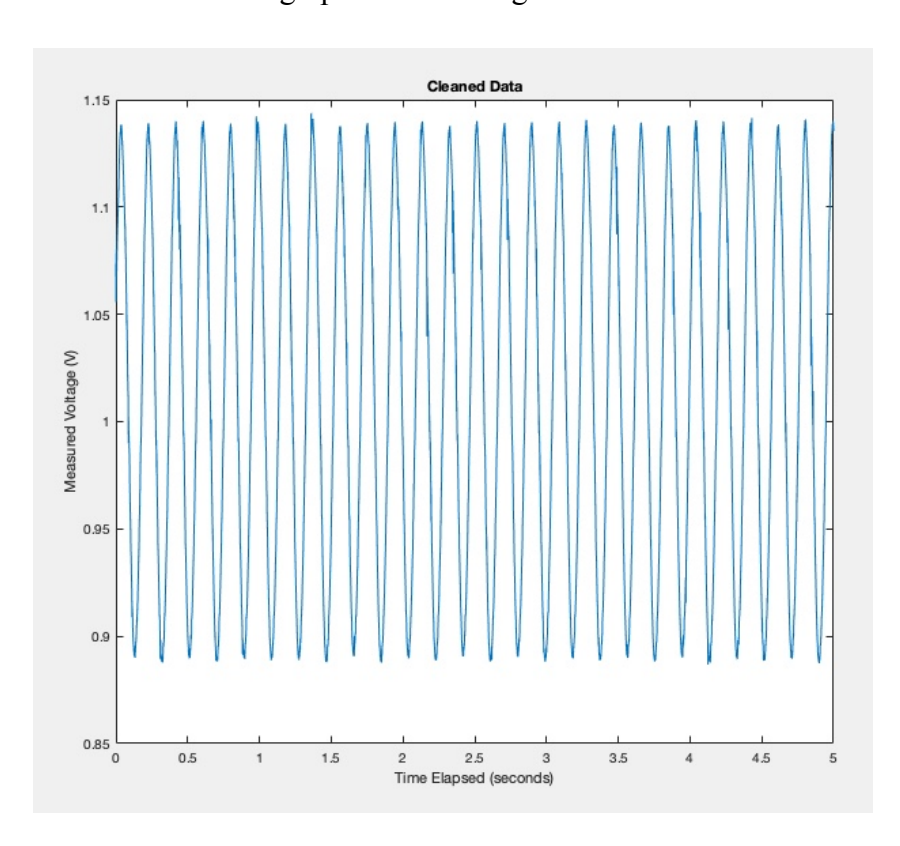


Figure 10: The output of a hampel filter applied to the data for 60% power

Upon successfully implementing the digital filter, most of the signal processing has been completed. The following manipulation resembles closely to the steps taken for the step-input function response, where the mean of the data was calculated and used to normalize the the data onto the x-axis, as well as taking the absolute value of the data set to invert all peaks onto one quadrant. This manipulated form of the data, as seen in Figure 11, signifies the final preparation before applying a "findpeaks" function to solve for the amplitude of each dataset at each frequency.

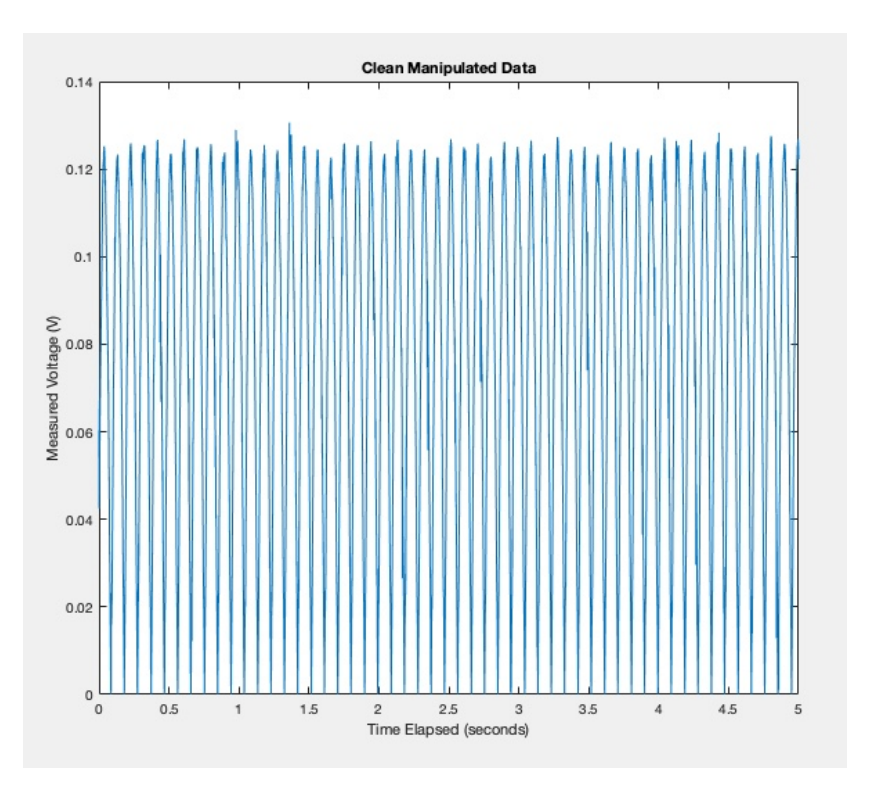


Figure 11: The final manipulated form of the sinusoidal data for 60% power

The following figure depicts a visual representation of what the "findpeaks" function calculates, and the mean amplitude value of each of all orange circles provided an accurate estimation of the mean amplitude of the second-order system response at each given frequency.

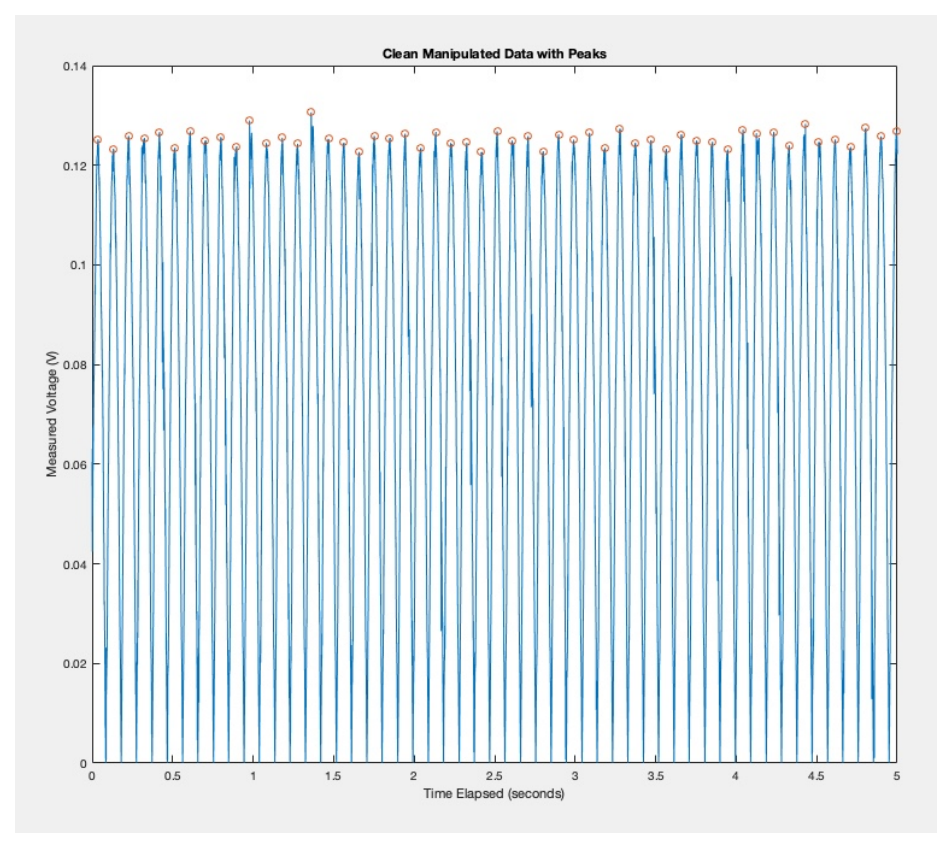


Figure 12: The "findpeaks" function clearly depicting the amplitude of the data set

After applying the aforementioned processes to all frequencies, the effective experimental amplitudes were divided by the input amplitude, known as  $X_B$ , to give a vector of amplitude ratios. These values were plotted over a range of frequencies ratios ( $w/w_n$ ) to give a final graph resulting in the relationship between magnitude and frequency. Uncertainty was introduced in terms of error bars, and is described in detail in the following section.

### **Uncertainty Analysis**

For this lab, we needed to perform an uncertainty analysis for the linear system calibration for the position vs voltage data collected. Because the voltage measured was collected by the computer in samples of 500000 for 5 seconds, the standard deviations were also automatically calculated which we used in the uncertainty analysis. All sample calculations shown are using the first values from the first trial or the average values. The sample calculations shown below are the calculations needed to calculate the  $y_{fit}$  values using the calculated calibration values for  $a_1$  and  $a_0$ . From these values for each of the six masses used in calibration, we solved for the standard deviation using the formula also shown in the sample calculation below. Using the standard deviations and t-values (determined by the number of samples taken - 2 which was 499998), the uncertainty came out to be  $\pm 0.00000599$  V [95%].

$$y_{fit} = x_{i} \cdot a_{i} + a_{0} = (0.356)(2.75 V_{m}) - 0.0713 V = 0.9065 V$$

$$56x = \sqrt{\frac{\Sigma(y_{fit} - 3meas)^{2}}{V}} = \sqrt{\frac{0.000004677}{499998}} = 0.000003058$$

$$V_{p,y_{fit}} = \frac{5}{5}x \cdot t_{v,q_{5}} = 0.000003058 \cdot 1.96 \approx 10.00000599 V \left[9696\right]$$

Using the calculated inverted  $a_1$  value, we were able to propagate the random uncertainty of the  $y_{fit}$  values from volts to millimeters as shown in the sample calculation below.

In the following sample calculation, the systematic uncertainty of the ADC's resolution was calculated to be  $\pm 0.000075$  V. Using error propagation, the total uncertainty in volts was calculated to be  $\pm 0.0000752$  V. To convert the total uncertainty of the calibration curve from

volts to millimeters, the total uncertainty in volts was multiplied by the inverted  $a_1$  value to get a total uncertainty value for the calibration curve of  $\pm 0.0000274$  mm.

After calculating the total uncertainty of the calibration curve, uncertainties of the second order response variables are needed to be calculated. As shown in the sample calculation below, the uncertainty of the damping frequency,  $w_d$ , was calculated using the four samples that we used for finding the damping ratio, the standard deviation of the four samples, and the t-value associated with the number of samples. The uncertainty of the damping frequency was calculated to be  $\pm 0.364$  rad/s. The uncertainty of the time constant was calculated by the number of peaks, the standard deviation and t-value which came out to be  $\pm 0.0345$ s. Using these two uncertainties with Equation 9 from above, the uncertainty of the damping ratio can be calculated. The partial derivative of Equation 9 was calculated with respect to the damping ratio and the time constant while multiplying by their respective damping ratio and time constant uncertainties for the error propagation used in the uncertainty below. The uncertainty of the damping ratio came out to be  $\pm 0.0123$  [95%].

K1:	107.23
K2:	100.98
K3:	93.47
K4:	92.26
K5:	96.39
Average k:	98.066
Std k:	6.126012569
Up,k:	7.588792017
Mass of weight (kg	0.12695
Uc part 1:	0.08686839049
Uc part 2:	0.03277834841
Uc,tot:	0.09284684911

**Table 5:** Raw data and values for uncertainty of the spring constant, k.

Using the five spring constant trials from Table 5, we were able to calculate the random uncertainty by finding the standard deviation, number of samples, and the t-value associated with the number of samples. The uncertainty of the spring constant (k) was calculated to be  $\pm 7.59$  N/m. Using the spring constant uncertainty, damping ratio uncertainty, and Equation 10 (combined with Equation 11), the uncertainty of the damping constant was able to be calculated. In the error propagation shown in the sample calculation below, the partial derivatives of Equation 10 with respect to the damping ratio and spring constant were calculated. In Table 5, "Uc part 1" and "Uc part 2" represent the resulting value of the partial derivative of a variable multiplied by the uncertainty of that variable. The uncertainty of the damping constant, c, was calculated to be  $\pm 0.0928$  N<sup>2</sup>s<sup>2</sup>/m<sup>2</sup> [95%].

In the uncertainty calculation for the natural frequency, the error propagation uses the uncertainties of the damping ratio and damping frequency as well as the partial derivatives of Equation 5 with respect to the damping ratio and damping frequency. As shown in the sample calculation below, the uncertainty of the natural frequency was calculated to be  $\pm 0.369$  rad/s [95%].

### **Results**

The following plots depict the final relationships calculated and described throughout this lab report. The first plot is a visual representation of the calibration curve performed to fit the output of the potentiometer to a physical position parameter.

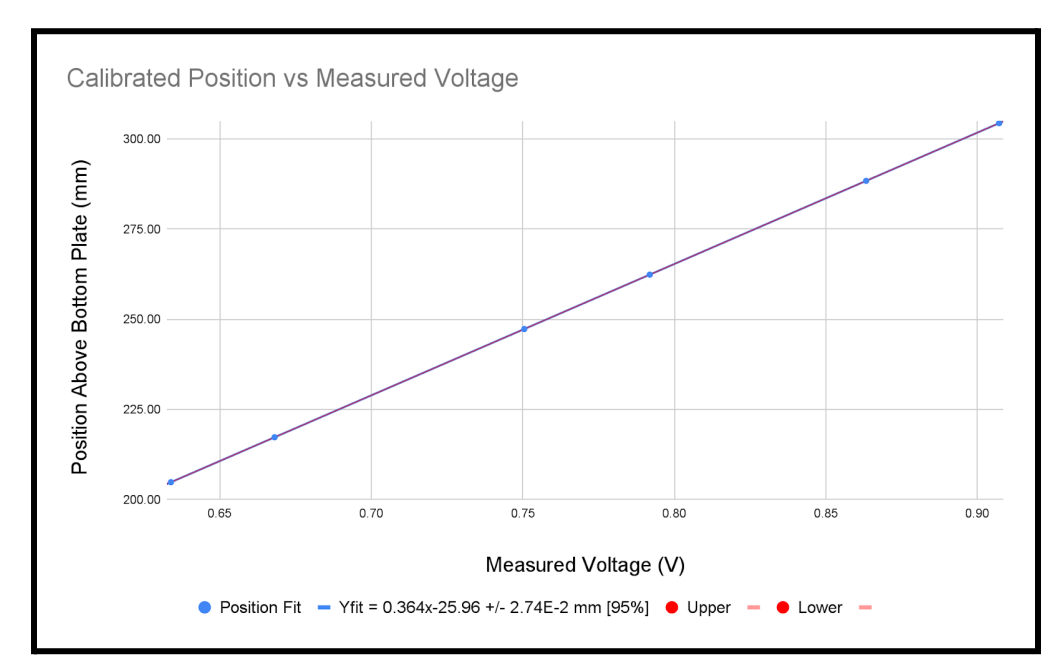


Figure 13: Measured position vs recorded voltage values from calibration with uncertainty bounds in red.

The next graph represents the time-dependent position of the top collar for four different frequencies. It is worth noting that the graphs include the original data as measured by the potentiometer and the filter data after applying digital signal processing, both of which have been converted into units of meters through the calculated calibration curve.

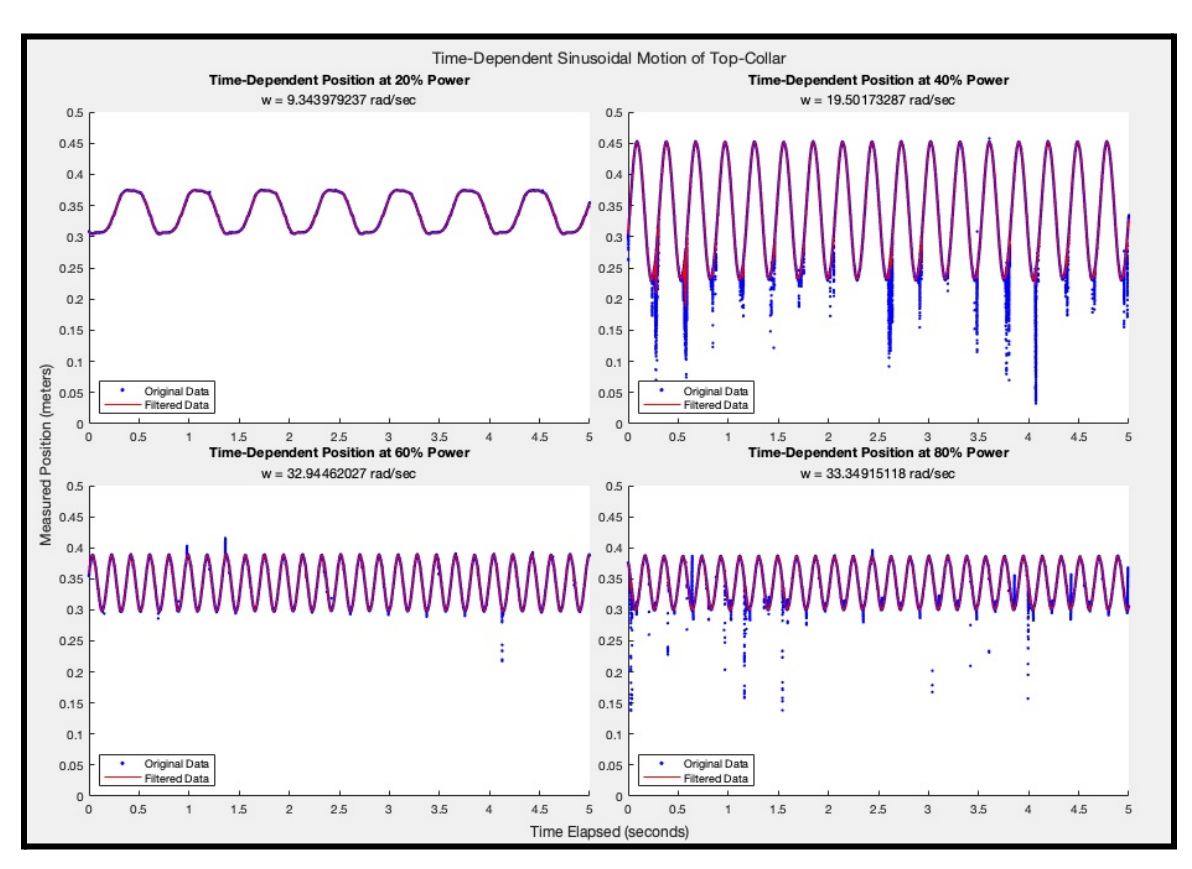


Figure 14: Raw data (blue) on the same plot as filtered data (red) for four select frequencies

The following graph plots the experimental amplitude ratio for all data sets, including distinction between increasing and decreasing increments, along with the theoretical frequency-dependent magnitude response based on experimental system parameters.

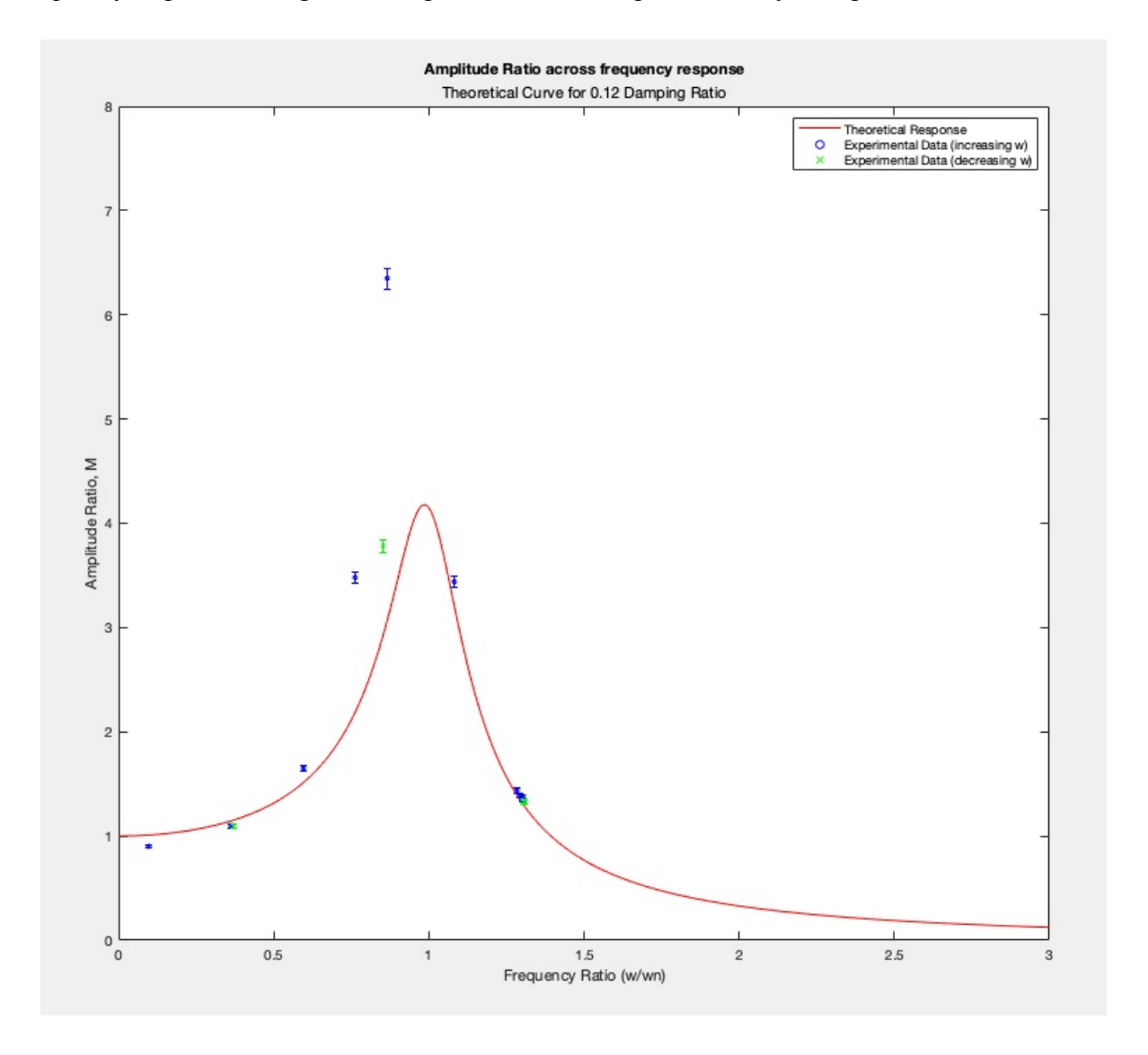


Figure 15: Theoretical Magnitude of the system plotted with experimental amplitude ratios at system frequencies

The following graph is shown to provide a clearer picture of the behavior of error and magnitude at the upper end of the frequency range that the system was capable of producing.

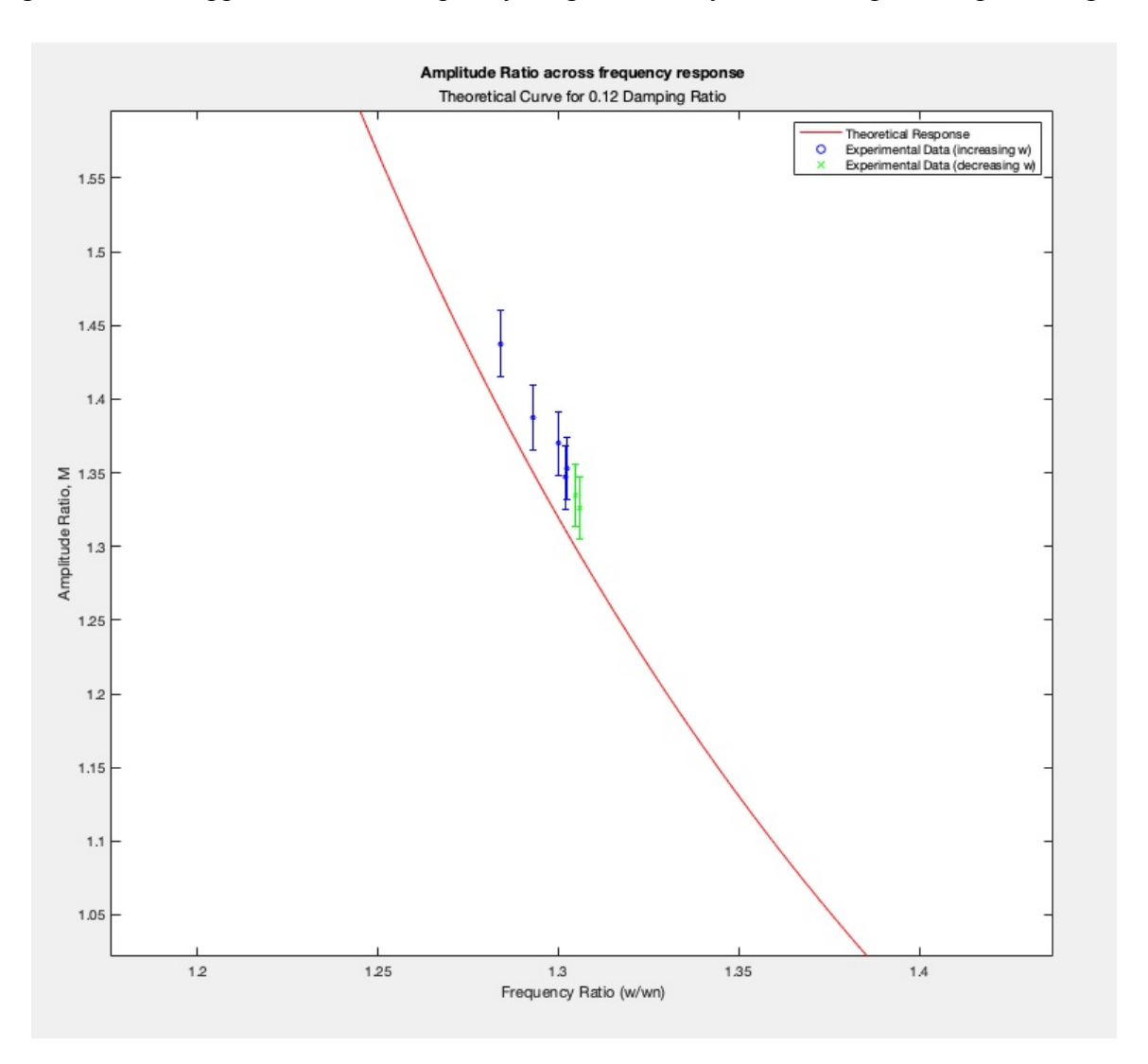


Figure 16: Enlarged upper frequency range to visualize constant-frquency cluster

The last plot depicts the theoretical phase shift of the second-order system as a function of the frequency domain.

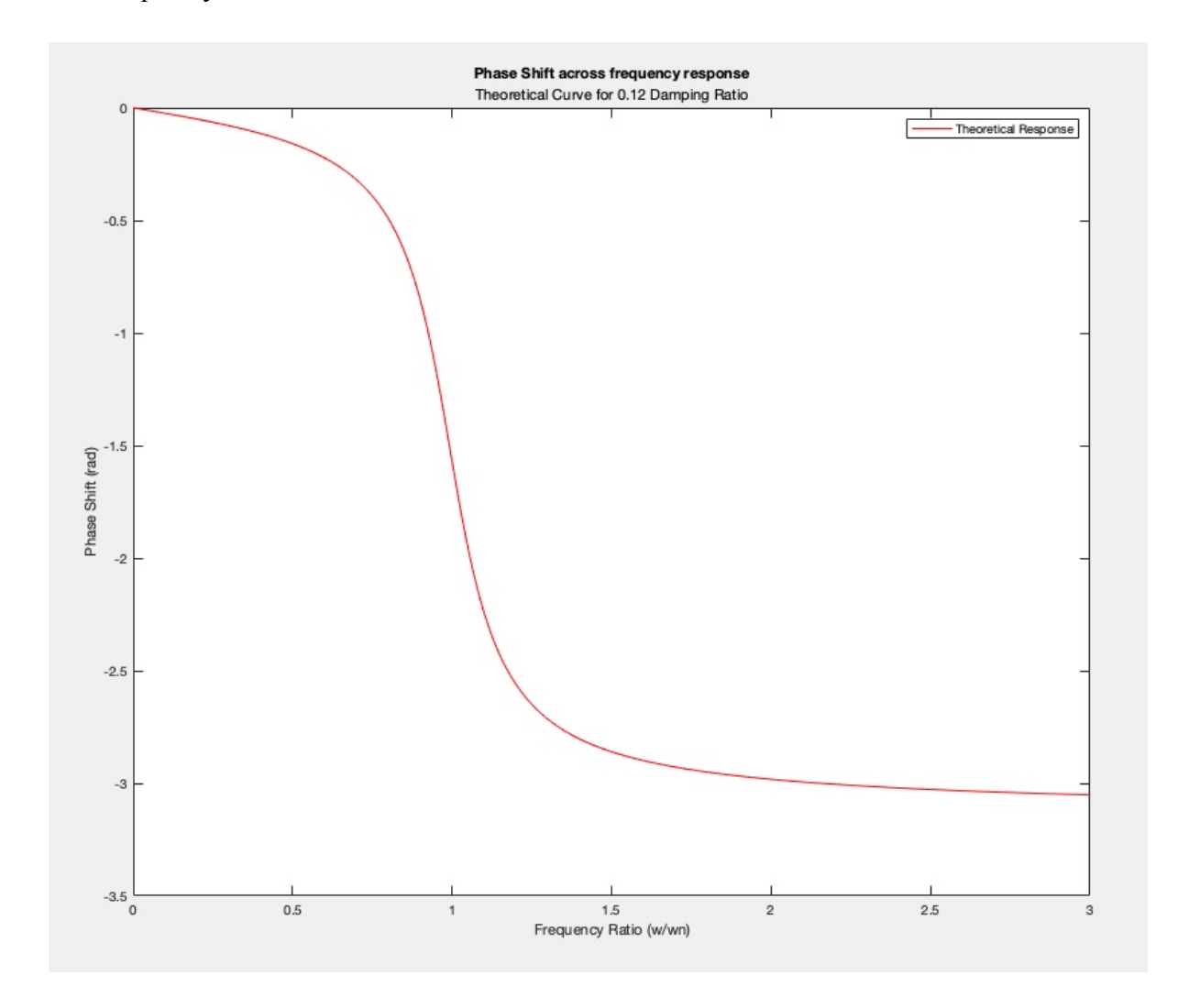


Figure 17: Theoretical phase shift of system at a damping ratio of 0.12

Lastly, a table of all system parameters, including uncertainty, shown below as a culmination of every analytical procedure performed in this lab.

Results:						
K:	98.066 +/- 7.589 (N/m) [95%]					
Wn:	24.8698 +/- 0.3689 (rad/s) [95%]					
Damping Ratio:	0.12 +/- 0.0123 [95%]					
c:	0.847 +/- 0.0928 (N^2*s^2/m^2) [95%]					
m:	0.127 (kg)					
K:	2.747 +/- 7.52E-5 (V/m) [95%]					
A:	0.0318 +/- 0.0005 (m) [95%]					
KA0 + O:	-0.0713 +/- 7.52E-5 (V) [95%]					

**Table 6:** Final results with uncertainty.

### **Discussion and Conclusion**

Looking at the parameters and descriptions this lab developed, there are some interesting features worth discussing. Firstly, nearly all the calculated uncertainty values for values in this system were quite small, usually under 10% of the nominal value. The best explanation for this comes from the extreme amount of data collected in each measurement. Collecting 500,000 data points per value is certainly overkill for simple measurements like the ones done in the calibration, but the benefit can't be denied. Having such a huge amount of data means that any amount of random uncertainty effectively rounds away due to significant figures, so effectively, all of the uncertainty comes straight from the measuring devices and other biased sources. This high confidence in the values is even shared with the spring constant uncertainty, which has an uncertainty value less than 10% despite only acquiring five values. While a large sample size doesn't apply to this particular calculation, the standard deviation between the five values was quite small, which resulted in a high confidence in this value as well.

The theoretical  $M(\omega)$  graph and the  $X/X_b$  plots found in Figure 15 both represent the same idea, though  $M(\omega)$  is modeled theoretically, while the  $X/X_b$  values were recorded experimentally. The first thing that pops out when viewing this graph is the difference between the maximum value for  $M(\omega)$  and the maximum experimental value. This difference is likely due to an overestimate of the damping ratio in the model. Q-analysis indicates a damping ratio of

0.08, which represents the model that would be developed from the experimental amplitude data, while this lab's other methods result in a value of .12 generated from step function analysis. This could have been caused by small variations in the experimental setup between when the step function data was collected and when the oscillatory data was collected. While their relationship has similar values at resonance (ignoring the resonance outlier), there is a notable gap between the two plots on the left side of the peak (before resonance frequency). For values *near* resonance, this offset would likely be due to the higher amount of uncertainty present for larger  $M(\omega)$  values. At these near resonant frequencies, the amplitude of the peaks would vary more, and thus the confidence in the amplitudes would be lower. For values far from resonance, this offset is likely due to the low amount of energy being applied to the system, which means that frictional effects represent a larger percentage of the system's interactions. This explanation also describes the flat-topped behavior of the 20% power graph seen in Figure 14, as the second mass was moving slow enough near the top and bottom of each oscillation that static friction likely took over and held the mass still before continuing to oscillate.

A quick note about the phase lag relationship seen in Figure 17, since nearly all the data points after 60% power had a frequency ratio  $(\omega/\omega_n)$  of ~1.4, these measurements should all be several radians out of phase. Unfortunately, there is no way to confirm this using the potentiometer sensor setup. Removing the top mass from the potentiometer setup was not an option in this lab, as there was a fear that it might damage the wire or connection. As a result, the actual input function of the bottom oscillator could not be measured to determine  $\Phi_0$ .

While this lab did produce quality data with good confidence intervals, there are still pieces of the procedure that could be improved upon. While the first two experimental setups (described in the Methods and Materials section) were an important part of the experimentation

process that ultimately led to the final setup, they were ultimately a result of rushing ahead instead of planning. Had the approach been more focused on theory for the first day and made fewer assumptions early on, multiple hours worth of useless data collection could have been prevented. Another issue present with this lab's procedure was the large gaps of data around the resonance frequency shown in Figure 15, an unfortunate result of the order this project took data in. All the data collection for an oscillating input was taken in one sitting, as the consistency of the wires and climate was determined to be more valuable than repeated sessions. A repercussion of this decision was that by the time data analysis began, it was too late to collect any more. With an opportunity to do things differently, collecting data in smaller increments and with redundancies around the resonance frequency would definitely be one of the main changes that could improve this procedure. Additionally, collecting more data on the downward trend would have provided a better understanding of potential hysteresis effects on the system. One final improvement that could have been made would be to also use more points to determine the spring constant of the system, k. This would reduce the uncertainty value for this parameter even more, providing more confidence in its calculation.

In terms of feedback for this lab, this group definitely felt a strong time crunch as the presentation and write up deadline got closer. Given the long time frame provided to complete this, and the large amount of effort the write up and subsequent presentation required, a recommended timeline that mentions key milestones would be a valuable resource for future lab groups. This tool could provide groups with a better understanding of their progress towards the final deadline, and help groups distribute the workload over the duration.

Ultimately, this lab tested many important skills from this class and industry that will prove extremely valuable moving forward. By designing and testing a sensor from scratch, this

lab taught valuable lessons on troubleshooting, iteration, and group design. Similarly, applying second order response knowledge to real world unfiltered data validated the usefulness of equations shown in class, substantiating the purpose of this lab further. With that being said, the objective of this lab was a clear success, even despite the large workload required to complete it.